

Table 2. Functional Evaluation of Gene Therapy

	GHG-lacZ	Naked FGF4	GHG-FGF4
Blood flow ratio (%) (ischemic/normal)			
Day 0 (BL)	33 ± 8 (6)	36 ± 11 (6)	37 ± 10 (6)
Day 38 (BL)	47 ± 12‡ (6)	58 ± 16‡ (6)	79 ± 16*‡§ (6)
Day 38 (Ad)	50 ± 12‡ (6)	68 ± 18‡ (6)	105 ± 13*†‡§ (6)
Angiographic score			
Day 38 (BL)	0.37 ± 0.12 (7)	0.39 ± 0.13 (7)	0.42 ± 0.11 (7)
Day 38 (Ad)	0.36 ± 0.10 (7)	0.41 ± 0.13 (7)	0.56 ± 0.15*†§ (7)
Blood pressure (%) (ischemic/normal)			
Day 10	31 ± 8 (6)	33 ± 5 (6)	26 ± 7 (6)
Day 38	56 ± 4 (6)	63 ± 6 (6)	70 ± 11* (6)

Angiographic score was calculated on the synchrotron radiation microangiogram. $p < 0.05$ vs. *GHG-lacZ, †naked FGF4, ‡day 0 (BL), and §day 38 (BL) (analysis of variance).

Ad = during adenosine administration; BL = under baseline condition; FGF4 = fibroblast growth factor 4; GHG = gelatin hydrogel; lacZ = β -galactosidase.

differences in baseline flow among the three groups were less marked than during adenosine administration.

Synchrotron radiation microangiography revealed microvessel responsiveness to the vasodilatory stimulation in the GHG-FGF4-treated rabbits (Figs. 4C and 4D), whereas vascular density was somewhat decreased by adenosine treatment in some of the GHG-lacZ-treated rabbits (Figs. 4A and 4B). Angiographic score analysis yielded quantitative evidence (Table 2). The angiographic score during adenosine administration (vasodilatory condition) was significantly higher in the GHG-FGF4 group (0.56 ± 0.15) than in either the naked FGF4-gene group (0.41 ± 0.13 , $p < 0.05$) or the GHG-lacZ group (0.36 ± 0.10 , $p < 0.05$, ANOVA). By contrast, under baseline conditions, the angiographic scores of the three groups were not significantly different.

On day 38, the GHG-FGF4 group had the highest calf-blood pressure ratio ($70 \pm 11\%$), and it was lower in the

naked FGF4-gene group ($63 \pm 6\%$), and even lower in the GHG-lacZ group ($56 \pm 4\%$, $p < 0.05$ vs. the GHG-lacZ group, ANOVA, Table 2). On day 10 (the time of gene transfer), the degrees of decrease in the three groups were not significantly different (26% to 33% in the mean).

Tissue damage was least in the GHG-FGF4-treated rabbits (Table 1). Limb muscle necrosis was $< 3 \text{ cm}^2$ and grade 1 or 2 in all of the animals in the GHG-FGF4 group, and significantly less than in the other two groups ($p < 0.05$, Kruskal-Wallis test). A similar difference was noted in the degrees of toe necrosis (data not shown). The muscle weight ratio (ischemic/normal) on day 38 was highest in the GHG-FGF4 group ($79 \pm 11\%$), lower in the naked FGF4-gene group ($62 \pm 14\%$), and even lower in the GHG-lacZ group ($48 \pm 6\%$), and the difference between the GHG-FGF4 group and GHG-lacZ group was significant ($p < 0.05$, ANOVA). The muscle weight ratio values (a morphological index) positively correlated with vascular responsiveness to adenosine (adenosine/baseline blood flow ratio [%]; a functional index) ($r = 0.50$, $n = 18$, $Sy \cdot x = 0.15$, $Sy \cdot x/y = 0.23$, $p = 0.045$). Thus, the blood flow, microangiographic, and morphologic analyses demonstrated a greater ameliorative effect of the GHG-FGF4 complex compared with the naked FGF4-gene (Tables 1 and 2).

Minimal inflammatory infiltrates, such as neutrophil and lymphoplasmacytic cell infiltrates, were noted at the injection site, but histological analysis showed that the infiltrates were localized. There was no evidence of fibrous proliferation or tumor formation in the transfected muscles or in other organs (right adductor muscle, stomach, liver, spleen, testes, kidneys, heart, lungs, and brain) in any of the groups.

DISCUSSION

We demonstrated that GHG potentiated the angiogenic effect of the FGF4-gene (protocol 2) by prolonging DNA degradation and improving transfection efficiency (protocol 1). Thus, GHG might facilitate the gene therapy of intractable circulatory disorders with genes for angiogenic growth factors.

Gelatin hydrogel augmented the effect of the FGF4-gene

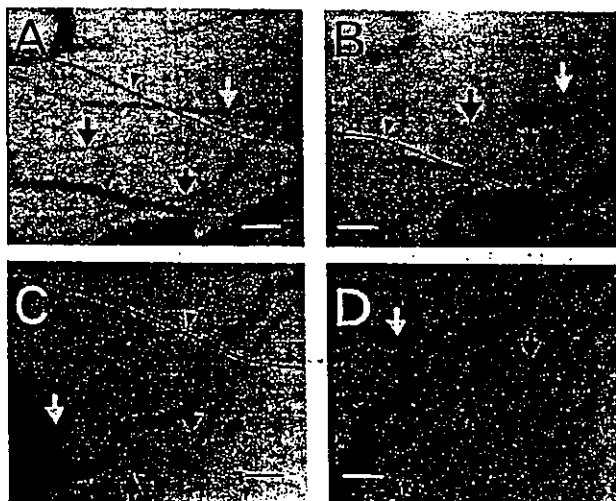


Figure 4. Representative synchrotron radiation microangiograms of the hindlimb ischemia in the rabbits. Synchrotron radiation microangiograms were taken under baseline conditions (A and C) and after repeated adenosine administration (B and D) on day 38. (A and B) Gelatin hydrogel (GHG)-lacZ-treated rabbit; (C and D) GHG-fibroblast growth factor 4-treated rabbit. Arrows indicate the same point in the vessels. Arrowheads reference copper wires with a diameter of $130 \mu\text{m}$; bar = 1 mm.

therapy by improving gene biodegradation and transfection efficiency. We demonstrated that GHG rapidly absorbed plasmid DNA and did not release it *in vitro* (see Methods section). In the radioiodine experiment, the radioactivity of naked DNA was reduced to less than 10% of the baseline within a day, whereas the radioactivity of DNA impregnated into GHG remained for four weeks (Fig. 1). In the experiment using the rabbit hindlimb ischemia model, the PCR analysis suggested that GHG expanded the gene transfer spatially (lanes 2 and 5 in Fig. 2). The maker gene experiment (protocol 1) confirmed that the use of GHG augmented both the number of transfected myocytes and the degree of gene expression in these cells, and also supported the spatially expanded gene expression (Fig. 3). The superiority of the therapeutic effects of the GHG-FGF4-gene complex on hindlimb ischemia compared with naked FGF4-gene treatment was confirmed in the rabbit experiments in protocol 2 (Fig. 4, Tables 1 and 2); GHG-FGF4-treated rabbits were characterized by less severe tissue damage in the ischemic limb (Table 2) and more marked vascular responsiveness to adenosine than either the naked FGF4-treated or GHG-lacZ-treated rabbits (Fig. 4, Table 2, Protocol 2 in the Results section). Under the baseline conditions, blood flow in normal muscle tissue is set at a relatively low level in preparation for an abrupt increase in flow demand (approximately 5× and 30× in the heart and in the skeletal muscle, respectively) during exercise, etc. (responsiveness to the vasodilatory stimulation). In other words, normal muscle tissue has a sufficient flow reserve (20,21), and, thus, the presence or absence of vascular responsiveness to adenosine administration can be used as an index of fundamental vascular function in angiogenic vascular segments. The demonstration of a positive correlation between flow responsiveness to adenosine and the muscle weight ratio further supports our hypothesis. Baseline flow may reflect the total number of angiogenic vessels, if it does not respond to vasodilatory stimulation. However, if the vasodilatory mechanism is present, baseline flow alone does not necessarily reflect the quality and/or quantity of angiogenic vascular segments. The amelioration of the ischemic tissue in the GHG-FGF4 group may be related to an adequate flow reserve (20,21) of so-called "well-tempered angiogenic vessels" (22).

Consequently, GHG offers several advantages as a new gene delivery system: 1) it has a positively charged structure, so it holds negatively charged nucleic acids, proteins, and drugs within its structure; 2) GHG is biodegradable and implantable; the biodegradable nature is from the gelatin itself but not from the hydrogel state. The substance bound to the GHG is gradually released as the gelatin degrades *in situ*. The degradation period can be adjusted to two to four weeks by varying the water content. Thus, the prolonged release of the DNA held in GHG was presumably responsible for the augmentation of gene therapy. The use of hydrogel-coated balloon-angioplasty-catheter has been reported (7). However, this gel is much different from our

hydrogel. The present GHG consists of amino acids and is biodegradable and implantable, whereas their hydrogel consists of carbohydrate and is not biodegradable nor implantable. 3) The isoelectric point and the shape of the GHG can be modified. Negatively charged GHG holds positively charged substances such as basic-FGF protein (6,23), and disk-shaped GHG has been found to be effective for reconstruction of bone defects (23); 4) GHG is less biohazardous than adenovirus vectors. Gelatin is already used in the clinical field, and its safety is established. Thus, the use of GHG with naked DNA improves its transfection efficiency without causing serious cytotoxicity or biohazards, which are inconvenient side effects of virus vectors (24). Therefore, the nonvirus vector GHG is useful for various gene therapies including the treatment of cardiovascular disorders.

Acknowledgments

The authors wish to thank Chiharu Tada, Akiko Hori, Sachie Ueno, and Takayuki Hasegawa for their technical work.

Reprint requests and correspondence: Dr. Hidezo Mori, Department of Cardiac Physiology, National Cardiovascular Center Research Institute, 5-7-1 Fujishirodai, Suita 565-8565, Japan. E-mail: hidemori@ri.ncvc.go.jp.

REFERENCES

1. Asahara T, Bauters C, Zheng LP, et al. Synergistic effect of vascular endothelial growth factor and basic fibroblast growth factor on angiogenesis *in vivo*. *Circulation* 1995;92:417-27.
2. Aoki M, Morishita R, Taniyama Y, et al. Angiogenesis induced by hepatocyte growth factor in non-infarcted myocardium and infarcted myocardium: up-regulation of essential transcription factor for angiogenesis. *Gene Ther* 2000;7:417-27.
3. Yang Y, Trinchieri G, Wilson JM. Recombinant IL-12 prevents formation of blocking IgA antibodies to recombinant adenovirus and allows repeated gene therapy to mouse lung. *Nat Med* 1995;1:890-3.
4. Zabner J, Ramsey BW, Meeker DP, et al. Repeat administration of an adenovirus vector encoding cystic fibrosis transmembrane conductance regulator to the nasal epithelium of patients with cystic fibrosis. *J Clin Invest* 1996;97:1504-11.
5. Takeshita S, Isshiki T, Sato T. Increased expression of direct gene transfer into skeletal muscles observed after acute ischemic injury in rats. *Lab Invest* 1996;74:1061-5.
6. Tabata Y, Hijikata S, Muniuzzaman M, Ikada Y. Neovascularization effect of biodegradable gelatin microspheres incorporating basic fibroblast growth factor. *J Biomater Sci Polym Ed* 1999;10:79-94.
7. Isner JM, Pieczek A, Schainfeld R, et al. Clinical evidence of angiogenesis after arterial gene transfer of phVEGF165 in patients with ischaemic limb. *Lancet* 1996;348:370-4.
8. Sakamoto H, Mori M, Taira M, et al. Transforming gene from human stomach cancers and a noncancerous portion of stomach mucosa. *Proc Natl Acad Sci USA* 1986;83:3997-4001.
9. Fuller PF, Peters G, Dickson C. Cell transformation by kFGF requires secretion but not glycosylation. *J Cell Biol* 1991;115:547-55.
10. Yoshida T, Ishimaru K, Sakamoto H, et al. Angiogenic activity of the recombinant hst-1 protein. *Cancer Lett* 1994;83:261-8.
11. Takeshita S, Zheng LP, Brogi E, et al. Therapeutic angiogenesis: a single intra-arterial bolus of vascular endothelial growth factor augments revascularization in a rabbit ischemic hind limb model. *J Clin Invest* 1994;93:662-70.
12. Miyazaki J, Takaki S, Araki K, et al. Expression vector system based on the chicken beta-actin promoter directs efficient production of interleukin-5. *Gene* 1989;79:269-77.

13. Bolton AE, Hunter WM. The labelling of proteins to high specific radioactivities by conjugation to a ^{125}I -containing acylating agent. *Biochem J* 1973;133:529-39.
14. Ueno H, Li JJ, Tomita H, et al. Quantitative analysis of repeat adenovirus-mediated gene transfer into injured canine femoral arteries. *Arterioscler Thromb Vasc Biol* 1995;15:2246-53.
15. Tanaka E, Hattan N, Ando K, et al. Amelioration of microvascular myocardial ischemia by gene transfer of vascular endothelial growth factor in rabbits. *J Thorac Cardiovasc Surg* 2000;120:720-8.
16. Tanioka K, Yamazaki J, Shidara K, et al. Avalanche-mode amorphous selenium photoconductive target for camera tube. *Adv Electronics Electron Phys* 1988;74:379-87.
17. Mori H, Hyodo K, Tanaka E, et al. Small-vessel radiography in situ with monochromatic synchrotron radiation. *Radiology* 1996;201:173-7.
18. Takeshita S, Isshiki T, Ochiai M, et al. Endothelium-dependent relaxation of collateral microvessels after intramuscular gene transfer of vascular endothelial growth factor in a rat model of hindlimb ischemia. *Circulation* 1998;98:1261-3.
19. Taira M, Yoshida T, Miyagawa K, Sakamoto H, Terada M, Sugimura T. cDNA sequence of human transforming gene hst and identification of the coding sequence required for transforming activity. *Proc Natl Acad Sci USA* 1987;84:2980-4.
20. Austin RJ, Aldea GS, Coggins DL, Flynn AE, Hoffman JI. Profound spatial heterogeneity of coronary reserve: discordance between patterns of resting and maximal myocardial blood flow. *Circ Res* 1990;67:319-31.
21. Coggins DL, Flynn AE, Austin RJ, et al. Nonuniform loss of regional flow reserve during myocardial ischemia in dogs. *Circ Res* 1990;67:253-64.
22. Biau H, Banfi A. The well-tampered vessel. *Nat Med* 2001;7:532-4.
23. Yamada K, Tabata Y, Yamamoto K, et al. Potential efficacy of basic fibroblast growth factor incorporated in biodegradable hydrogels for skull bone regeneration. *J Neurosurg* 1997;86:871-5.
24. Marshall E. Gene therapy death prompts review of adenovirus vector. *Science* 1999;286:2244-5.

Hybrid Cell–Gene Therapy for Pulmonary Hypertension Based on Phagocytosing Action of Endothelial Progenitor Cells

Noritoshi Nagaya, MD; Kenji Kangawa, PhD; Munetake Kanda, MD; Masaaki Uematsu, MD; Takeshi Horio, MD; Naoto Fukuyama, MD; Jun Hino, PhD; Mariko Harada-Shiba, MD; Hiroyuki Okumura, MD; Yasuhiko Tabata, PhD; Naoki Mochizuki, MD; Yoshihide Chiba, MD; Keisuke Nishioka, MD; Kunio Miyatake, MD; Takayuki Asahara, MD; Hiroshi Hara, MD; Hidezo Mori, MD

Background—Circulating endothelial progenitor cells (EPCs) migrate to injured vascular endothelium and differentiate into mature endothelial cells. We investigated whether transplantation of vasodilator gene-transduced EPCs ameliorates monocrotaline (MCT)-induced pulmonary hypertension in rats.

Methods and Results—We obtained EPCs from cultured human umbilical cord blood mononuclear cells and constructed plasmid DNA of adrenomedullin (AM), a potent vasodilator peptide. We used cationic gelatin to produce ionically linked DNA-gelatin complexes. Interestingly, EPCs phagocytosed plasmid DNA-gelatin complexes, which allowed nonviral, highly efficient gene transfer into EPCs. Intravenously administered EPCs were incorporated into the pulmonary vasculature of immunodeficient nude rats given MCT. Transplantation of EPCs alone modestly attenuated MCT-induced pulmonary hypertension (16% decrease in pulmonary vascular resistance). Furthermore, transplantation of AM DNA-transduced EPCs markedly ameliorated pulmonary hypertension in MCT rats (39% decrease in pulmonary vascular resistance). MCT rats transplanted with AM-expressing EPCs had a significantly higher survival rate than those given culture medium or EPCs alone.

Conclusions—Umbilical cord blood–derived EPCs had a phagocytosing action that allowed nonviral, highly efficient gene transfer into EPCs. Transplantation of AM gene-transduced EPCs caused significantly greater improvement in pulmonary hypertension in MCT rats than transplantation of EPCs alone. Thus, a novel hybrid cell–gene therapy based on the phagocytosing action of EPCs may be a new therapeutic strategy for the treatment of pulmonary hypertension. (*Circulation*. 2003;108:889-895.)

Key Words: pulmonary heart disease ■ natriuretic peptides ■ gene therapy ■ endothelium

The pulmonary endothelium plays an important role in the regulation of pulmonary vascular tone through the release of vasoactive substances such as nitric oxide, prostacyclin, and adrenomedullin (AM).¹ Dysfunction of the endothelium may play a role in the pathogenesis of pulmonary hypertension, including primary pulmonary hypertension.² Thus, pulmonary endothelial cells may be a therapeutic target for the treatment of pulmonary hypertension. Recently, endothelial progenitor cells (EPCs) have been discovered in adult peripheral blood.³ EPCs are mobilized from bone marrow into the peripheral blood in response to tissue ischemia or traumatic injury, migrate to sites of injured

endothelium, and differentiate into mature endothelial cells in situ.^{4–6} These findings raise the possibility that transplanted EPCs may serve not only as a tissue-engineering tool to reconstruct the pulmonary vasculature but also as a vehicle for gene delivery to injured pulmonary endothelium.

We prepared biodegradable gelatin that could hold negatively charged protein or plasmid DNA in its positively charged lattice structure.^{7,8} We have shown that the gelatin is promptly phagocytosed and then gradually degraded by phagocytes, including macrophages.⁹ However, whether EPCs phagocytose ionically linked plasmid DNA-gelatin complexes remains unknown. If this is the case, the phago-

Received December 3, 2002; revision received April 17, 2003; accepted April 18, 2003.

From the Departments of Internal Medicine (N.N., T.H., K.M.) and Perinatology (Y.C.), National Cardiovascular Center, Osaka, Japan; Departments of Biochemistry (K.K., J.H., M.H.-S., H.O.), Cardiac Physiology (M.K., H.M.), and Structural Analysis (N.M.), National Cardiovascular Center Research Institute, Osaka, Japan; Cardiovascular Division (M.U.), Kansai Rosai Hospital, Hyogo, Japan; Department of Physiology (N.F.), Tokai University School of Medicine, Kanagawa, Japan; Department of Biomaterials (Y.T.), Field of Tissue Engineering, Institute for Frontier Medical Sciences, Kyoto University, Kyoto, Japan; Department of Transfusion Medicine (K.N., H.H.), Hyogo College of Medicine, Hyogo, Japan; and Department of Regenerative Medicine (T.A.), Institute of Biomedical Research and Innovation, Kobe, Japan.

Reprint requests to Noritoshi Nagaya, MD, or Hidezo Mori, MD, Department of Internal Medicine, National Cardiovascular Center, 5-7-1 Fujishirodai, Suita, Osaka 565-8565, Japan. E-mail nagayann@hsp.nccv.go.jp or hidemori@ri.nccv.go.jp

© 2003 American Heart Association, Inc.

Circulation is available at <http://www.circulationaha.org>

DOI: 10.1161/01.CIR.0000079161.56080.22

cytic activity of EPCs would allow nonviral gene transfer into EPCs. Here we provide rationale of a novel hybrid cell-gene therapy for pulmonary hypertension.

AM is a potent vasodilator peptide that was originally isolated from human pheochromocytoma.¹ There are abundant binding sites for AM in the pulmonary vasculature.¹⁰ The plasma AM level increases in proportion to the severity of pulmonary hypertension, and circulating AM is partially metabolized in the lungs.¹¹ Recently, we have shown that intravenous administration of AM significantly decreases pulmonary vascular resistance in patients with heart failure or primary pulmonary hypertension.^{12,13} These findings suggest that AM plays an important role in the regulation of pulmonary vascular tone. Thus, we hypothesized that transplantation of AM DNA-transduced EPCs would improve monocrotaline (MCT)-induced pulmonary hypertension. To test this hypothesis, we investigated whether EPCs phagocytose DNA-gelatin complexes, which would allow nonviral gene transfer into EPCs; whether intravenously administered EPCs are incorporated into the pulmonary vasculature; and whether transplantation of AM DNA-transduced EPCs ameliorates MCT-induced pulmonary hypertension and improves survival in MCT rats.

Methods

Culture of EPCs

Human umbilical cord blood mononuclear cells were plated on fibronectin-coated dishes and cultured in Medium 199 supplemented with 20% FBS, bovine pituitary extract, vascular endothelial growth factor, basic fibroblast growth factor, heparin, and antibiotics, as reported previously.^{3,6,14} On days 4 and 8 of culture, nonadherent cells were removed, and medium was replaced. All mothers gave written informed consent, and the study was approved by the ethics committee.

Fluorescent Staining for EPCs

Adherent cells on day 8 of culture were stained by acetylated LDL labeled with DiI (DiI-acLDL, Biomedical Technologies) and fluorescein isothiocyanate (FITC)-labeled lectin from *Ulex europaeus* (Sigma). Double-positive cells for DiI-acLDL and FITC-labeled lectin were identified as EPCs, as reported previously.^{15,16}

Flow Cytometry

Adherent cells on day 8 of culture and green fluorescent protein (GFP) gene-transduced cells were analyzed by fluorescence-activated cell sorting (FACS; FACS SCAN flow cytometer, Becton Dickinson). Cells were incubated for 30 minutes at 4°C with phycoerythrin-conjugated mouse monoclonal antibodies against human CD14 (clone M5E2), CD31 (clone L133.1), CD68 (clone Y1/82A), and CD83 (clone HB15e; all from Becton Dickinson) and mouse monoclonal antibodies against human KDR (clone KDR-1, Sigma) and VE-cadherin (clone BV6, Chemicon). Isotype-identical antibodies served as controls.

Preparation of Biodegradable Gelatin and Plasmid DNA

We prepared biodegradable cationic gelatin, as a matrix to hold plasmid DNA, as reported previously.⁷ In brief, a gelatin sample with an isoelectric point of 9.0 was isolated from bovine bone collagen. Gelatin microspheres were prepared through the glutaraldehyde cross-linking of gelatin. The microspheres were washed with acetone and distilled water and then freeze-dried. We constructed the pcDNA1.1-CMV vector (Invitrogen) encoding human AM cDNA or GFP cDNA. The gelatin (5 to 30 μm in diameter, 2 mg) was added

to plasmid DNA (200 $\mu\text{g}/200 \mu\text{L}$ in PBS, pH 7.4). After 24-hour incubation at 4°C, DNA-gelatin complexes were obtained.

Ex Vivo Gene Transfer Into EPCs

EPCs (5×10^5) were cultured with ionically linked GFP or AM DNA-gelatin complexes (200 $\mu\text{g}/2 \text{ mg}$) for 72 hours. To examine DNA localization, AM plasmid DNA was labeled by rhodamine B isothiocyanate (RITC), as reported previously.⁸ The nuclei of EPCs were stained by DAPI (Sigma). Immunocytochemistry for AM was performed with a mouse monoclonal antibody against human AM-(46-52). Human AM level in culture medium ($n=5$) was measured by radioimmunoassay.

Assay for AM

The culture medium and lung tissues were acidified with acetic acid, boiled to inactivate intrinsic proteases, and lyophilized. Human AM levels in culture medium, lung tissues, and plasma were measured with a radioimmunoassay kit (Shionogi).¹²

In Vivo Experimental Protocol

Male immunodeficient (F344/N *nu/nu*) nude rats weighing 100 to 120 g were randomly assigned to receive a subcutaneous injection of 60 mg/kg MCT or 0.9% saline. Seven days after MCT injection, 1×10^6 EPCs, 1×10^6 AM-expressing EPCs, or culture medium (500 μL each) was administered intravenously via the left jugular vein. Sham rats also received intravenous administration of 500 μL of culture medium. We used 1×10^6 cells per rat to obtain maximal effects of transplanted EPCs on the basis of dose-response experiments. This protocol resulted in the creation of 4 groups: MCT rats given EPCs (EPC group, $n=8$), MCT rats given AM-expressing EPCs (AM-EPC group, $n=9$), MCT rats given culture medium (control group, $n=9$), and sham rats given culture medium (sham group, $n=8$). Human mature pulmonary artery endothelial cells served as control cells.

Hemodynamic studies were performed 3 weeks after MCT injection. A polyethylene catheter was inserted into the right femoral artery. An umbilical vessel catheter was inserted through the right jugular vein into the pulmonary artery. Cardiac output was measured in triplicate by the thermodilution method. Pulmonary vascular resistance was calculated by dividing mean pulmonary arterial pressure by cardiac output.

Immunohistochemical and Immunofluorescence Staining

Immunohistochemistry was performed on paraformaldehyde-fixed, paraffin-embedded 5- μm sections of the lungs. To discern human endothelial cells from rat cells, we used mouse anti-human CD31 (DAKO) and mouse anti-rat CD31 (BD PharMingen) monoclonal antibodies. The sections were sequentially developed for the peroxidase and alkaline phosphatase substrates. Immunofluorescence staining for rat CD31 was performed on frozen sections with mouse anti-rat CD31 monoclonal antibody (BD PharMingen) and RITC-conjugated anti-mouse IgG antibody (DAKO).

Morphometric Analysis of Pulmonary Arteries

We analyzed the medial wall thickness of the pulmonary arteries in the middle region of the right lung (20 muscular arteries/rat, ranging in external diameter from 25 to 50 and from 51 to 100 μm). The medial wall thickness was expressed as follows: % wall thickness = [(medial thickness $\times 2$) / external diameter] $\times 100$.

Survival Analysis

Seven days after MCT injection, 29 rats received intravenous injection of 1×10^6 EPCs (EPC group, $n=10$), 1×10^6 AM-expressing EPCs (AM-EPC group, $n=10$), or culture medium (control group, $n=9$). Survival was estimated from the date of MCT injection to the death of the rat or 10 weeks after transplantation.

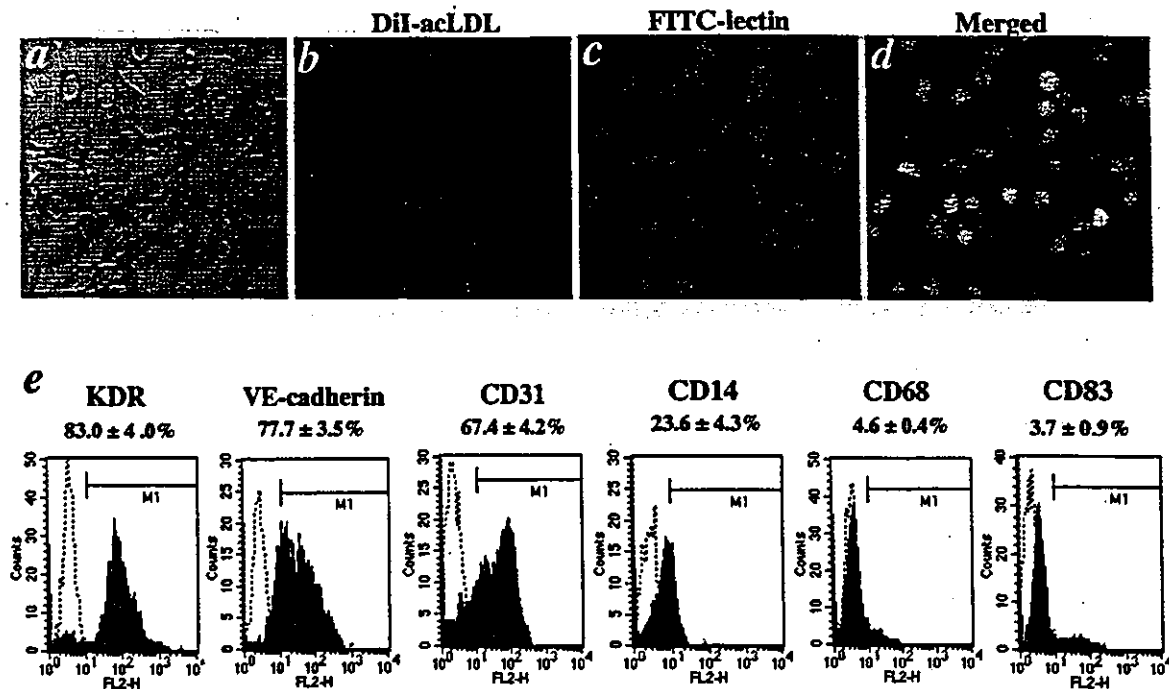


Figure 1. Characterization of EPCs derived from human umbilical cord blood. EPCs exhibited spindle-shaped or cobblestone-like morphology (a) and took up DiI-acLDL and FITC-labeled lectin in same field (b–d). e, Flow cytometric analysis of adherent cells on day 8. Most of adherent cells expressed endothelial lineage markers (KDR, VE-cadherin, and CD31), whereas they were negative for CD68 and CD83.

Statistical Analysis

Data were expressed as mean \pm SEM. Comparisons of parameters among the 4 groups were made by 1-way ANOVA, followed by the Scheffe multiple comparison test. Comparisons of the time course of parameters between the 2 groups were made by 2-way ANOVA for repeated measures, followed by the Scheffe multiple comparison test. Survival curves were derived by the Kaplan-Meier method and compared with log-rank tests. A probability value <0.05 was considered statistically significant.

Results

EPCs From Human Umbilical Cord Blood

After 8-day culture of mononuclear cells, spindle-shaped or cobblestone-like adherent cells were observed (Figure 1a). Most of the adherent cells were double stained by DiI-acLDL and FITC-labeled lectin (Figure 1b, c, and d). These cells expressed endothelial cell-specific antigens (KDR, VE-cadherin, and CD31; Figure 1e). In contrast, the majority of adherent cells were negative for monocyte/macrophage marker CD68 and dendritic cell marker CD83. Although a small fraction of the adherent cells expressed monocyte marker CD14, this marker has been shown to also be expressed on activated endothelial cells and cultured EPCs.¹⁷ Thus, we confirmed that the major population of the adherent cells were EPCs.

Phagocytosis of DNA-Gelatin Complex by EPCs

EPCs were cultured with GFP DNA-gelatin complexes (Figure 2a). Interestingly, GFP was expressed in EPCs after 72-hour incubation (Figure 2b). Quantitative analyses by FACS confirmed a high incidence ($76 \pm 3\%$, $n=5$) of GFP expression in adherent cells. KDR/GFP double-positive cells

made up $70 \pm 2\%$ of the adherent cells, whereas CD68/GFP double-positive cells accounted for $2 \pm 1\%$ (Figure 2c). Transmission electron microscopy demonstrated that EPCs were phagocytosing DNA-gelatin complexes (Figure 2d). These results suggest that EPCs phagocytose DNA-gelatin complexes in coculture, which allows nonviral, highly efficient gene transfer into EPCs. Unlike gelatin, cationic liposome-mediated transfection efficiency was low ($24 \pm 3\%$).

A number of DNA particles labeled by RITC were incorporated into gelatin (Figure 2e). RITC-labeled DNA particles were gradually released from gelatin within EPCs through gelatin degradation (Figure 2f). After 72-hour incubation, RITC-labeled DNA particles released from gelatin were distributed in the cytoplasm of EPCs (Figure 2g). These results suggest the ability of EPCs to take up DNA-gelatin complexes and dissolve the gelatin, freeing the DNA into EPCs. Unlike EPCs, human mature pulmonary artery endothelial cells did not phagocytose DNA-gelatin complexes.

When EPCs were cultured with AM DNA-gelatin complexes, intense immunostaining for AM was observed in EPCs impregnated with AM DNA-gelatin (Figure 3a). After 72-hour incubation, EPCs markedly secreted AM into the culture medium (10-fold increase compared with EPCs alone; Figure 3b). AM overproduction lasted for more than 16 days after gene transfer. AM secretion from EPCs was not influenced by the presence of gelatin (data not shown).

Incorporation of EPCs Into the Pulmonary Vasculature

GFP-expressing EPCs were administered intravenously 7 days after MCT injection. Three days after transplantation,

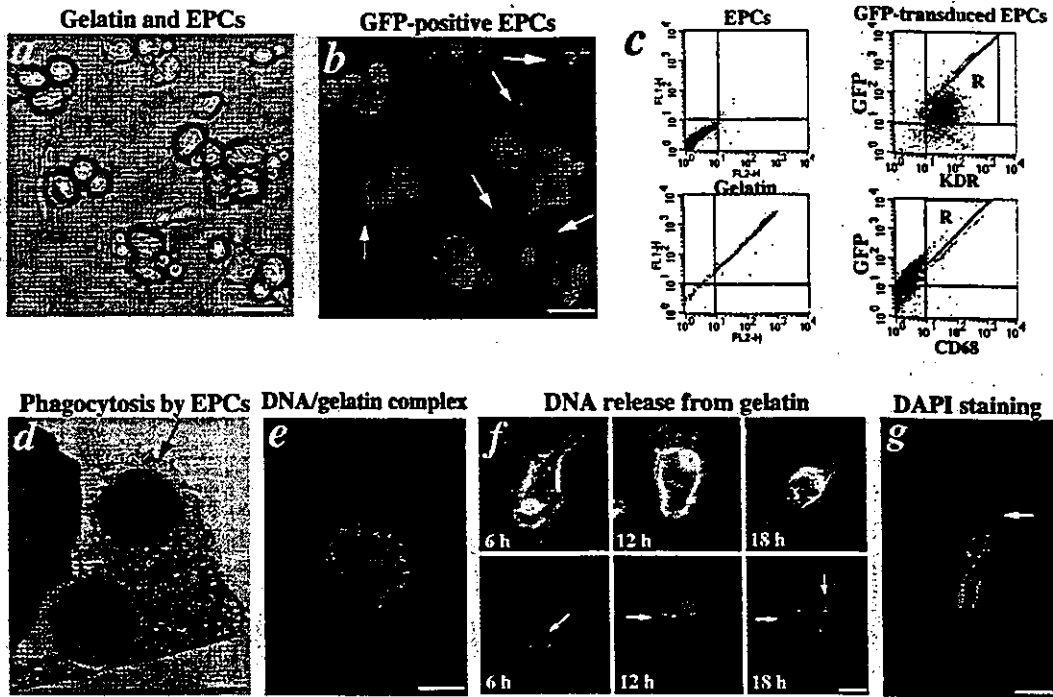


Figure 2. Ex vivo gene transfer into EPCs based on phagocytosing action. a, EPCs were cultured with ionically linked GFP DNA-gelatin complexes. b, GFP was highly expressed in EPCs (arrows) in same field as Figure 2a. c, Flow cytometric analyses of EPCs cultured with GFP DNA-gelatin complexes. Negative controls (EPC isocontrol and gelatin background) are shown in left panels. d, Transmission electron microscopy revealed that EPCs had phagocytosed GFP DNA-gelatin complexes (arrows). e, RITC-labeled DNA particles were incorporated into gelatin. f, RITC-labeled DNA particles (red, arrows) were released from gelatin through its degradation. g, RITC-labeled DNA particles released from gelatin (arrow) were distributed in cytoplasm of EPCs. Nuclei of EPCs were identified by DAPI staining. Scale bars: 10 μ m (a and b); 2 μ m (d and e); 5 μ m (f and g).

GFP-expressing EPCs were incorporated into the walls of pulmonary arterioles in MCT rats and composed pulmonary vasculature (Figure 4a). Transplanted GFP-expressing EPCs were distributed on lung tissues (Figure 4b). AM gene-transduced EPCs were similarly incorporated into the pulmonary vasculature (Figure 4c). Immunohistochemical analyses of rat and human CD31 demonstrated that the transplanted EPCs were of endothelial lineage and comprised a vessel structure similar to rat endothelial cells (Figure 4c). However, transplanted EPCs were rarely distributed to other tissues such as cardiac ventricles, kidneys, aorta, and brain (data not shown).

Effects of Gene-Transduced EPC Transplantation on Pulmonary Hypertension

Pulmonary hypertension developed 3 weeks after MCT injection. Mean pulmonary arterial pressure was not strikingly decreased in the EPC group (-14%) but was significantly lower in the AM-EPC group (-29%) than in the control group (Figure 5a). Pulmonary vascular resistance was significantly lower in both the EPC group (-16%) and the AM-EPC group (-39%) than in the control group (Figure 5b). Importantly, the AM-EPC group showed significantly greater improvement in pulmonary vascular resistance than the EPC group. Right ventricular weight and right ventricular

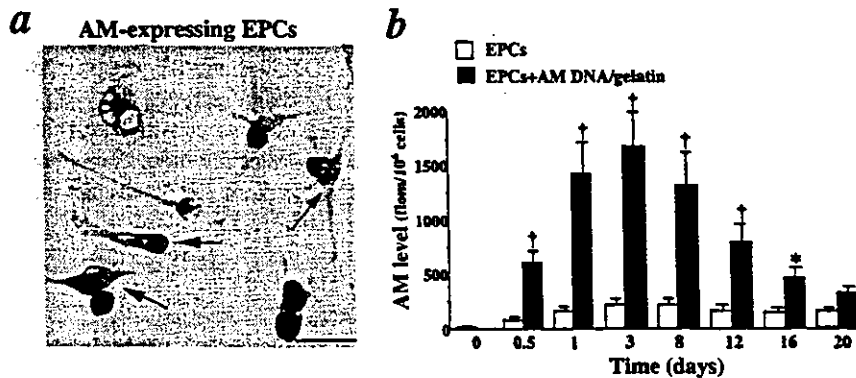


Figure 3. AM gene transfer into EPCs. a, Immunohistochemical analysis of AM in EPCs after gene transfer. Intense immunostaining for AM was observed in EPCs (arrows). Scale bar: 10 μ m. b, Time course of AM secretion from EPCs during coculture with AM DNA-gelatin complexes. Data are mean \pm SEM. * P <0.05, † P <0.001 vs EPCs.

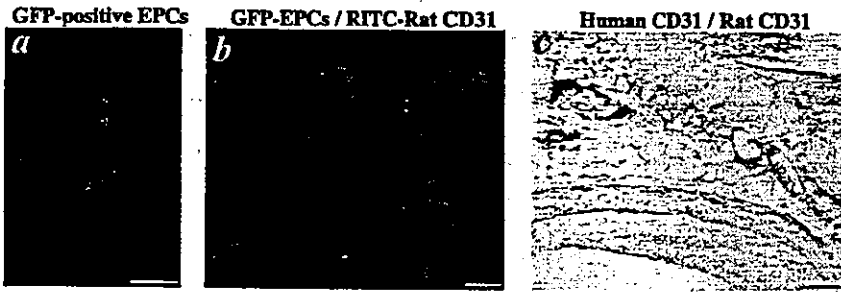


Figure 4. Distribution of EPCs in lungs of MCT rats. a, Intravenously administered GFP-expressing EPCs were incorporated into walls of pulmonary arterioles. b, Transplanted GFP-expressing EPCs were distributed on lung tissues. Pulmonary vasculature was detected by RITC-conjugated anti-rat CD31 (red). c, Immunohistochemistry for human CD31 (peroxidase, brown) and rat CD31 (alkaline phosphatase, pink). Scale bars: 50 μ m.

systolic pressure were significantly lower in the AM-EPC group than in the control and EPC groups (Table). AM levels in plasma and lung tissues were significantly higher in the AM-EPC group than in the other groups 2 weeks after transplantation. Unlike EPCs, transplantation of mature pulmonary artery endothelial cells did not significantly influence pulmonary hemodynamics in MCT rats.

Representative photomicrographs showed that hypertrophy of the pulmonary vessel wall after MCT injection was attenuated in both the EPC and AM-EPC groups (Figure 5c). Quantitative analysis also demonstrated a significant increase in percent wall thickness after MCT injection, but this change was markedly attenuated in the AM-EPC group (Figure 5d). Kaplan-Meier survival curves demonstrated that MCT rats transplanted with AM-expressing EPCs (AM-EPC group) had a significantly higher survival rate than those given culture medium (control group) or EPCs alone (EPC group; Figure 5e).

Discussion

In the present study, we present a new concept for cell-based gene delivery into the pulmonary vasculature that consists of 3 processes. First, cationic gelatin is readily complexed with plasmid DNA. Second, EPCs phagocytose ionically linked plasmid DNA-gelatin complexes in coculture, which allows

nonviral gene transfer into EPCs with high efficiency. Third, transplanted gene-modified EPCs are incorporated into pulmonary vascular beds in MCT rats. This novel gene delivery system has great advantages over conventional gene therapy: nonviral, noninvasive, and highly efficient gene targeting into the pulmonary vasculature. These benefits may be achieved mainly by the ability of EPCs to phagocytose DNA-gelatin complexes and to migrate to sites of injured endothelium.

Tabata et al⁷ and Fukunaka et al⁸ demonstrated that gelatin can hold negatively charged protein or plasmid DNA in its positively charged lattice structure. In addition, Tabata et al⁹ demonstrated that gelatin is promptly phagocytosed and gradually degraded by macrophages. The present study first demonstrated that EPCs phagocytosed ionically linked DNA-gelatin complexes, dissolved gelatin, and freed the DNA. Surprisingly, the transfection efficiency of this approach was markedly high. FACS analysis demonstrated that EPCs, not monocytes/macrophages, are the main contributors of GFP expression. These findings suggest that the phagocytosing action of EPCs allows nonviral, highly efficient gene transfer into EPCs themselves.

Recently, intravenously administered hematopoietic cells have been shown to be attracted to sites of cerebral injury.¹⁸ Intravenously injected EPCs accumulate in ischemic myocar-

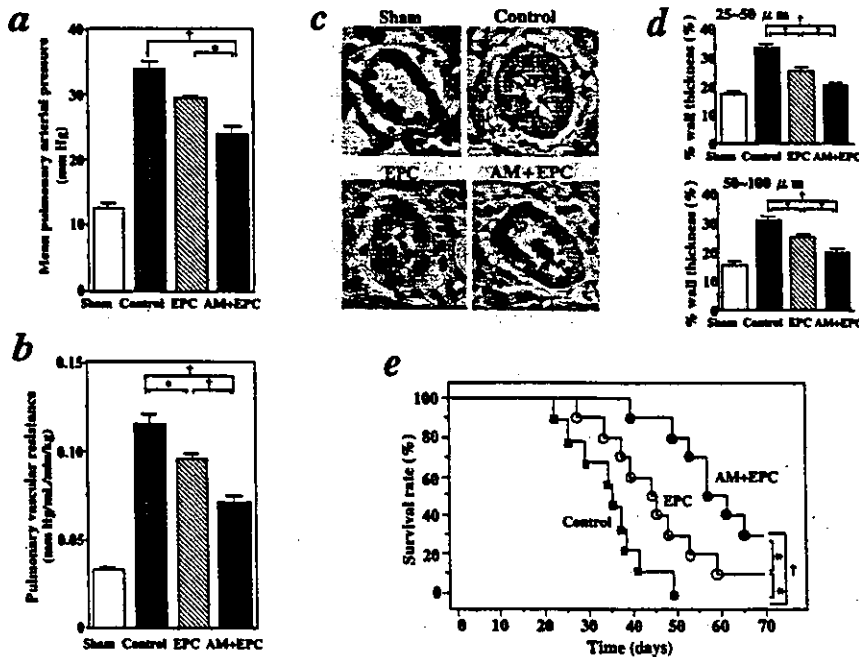


Figure 5. Effects of AM DNA-transduced EPC transplantation on mean pulmonary arterial pressure (a) and pulmonary vascular resistance (b) in MCT rats. c, Representative photomicrographs of peripheral pulmonary arteries in rats. Scale bars, 20 μ m. d, Quantitative analysis of percent wall thickness of peripheral pulmonary arteries. e, Kaplan-Meier survival curves of MCT rats transplanted with AM-expressing EPCs (AM-EPC group, ●), EPCs alone (EPC group, ○), or culture medium (control group, □). Data are mean \pm SEM. **P*<0.05; †*P*<0.001.

Physiological Profiles of 4 Experimental Groups

	Sham (n=8)	Control (n=9)	EPC (n=8)	AM-EPC (n=9)
Body weight, g	191±4	174±7	181±6	182±6
RV weight, g/kg body weight	0.59±0.02	1.04±0.05	0.91±0.03	0.77±0.04*†
Left ventricular weight, g/kg body weight	2.42±0.03	2.49±0.05	2.46±0.04	2.44±0.09
Heart rate, bpm	398±10	390±11	398±15	387±11
Mean arterial pressure, mm Hg	112±4	100±5	104±3	98±4
RV systolic pressure, mm Hg	32±2	63±3	56±1*	48±2*†
Plasma human AM, fmol/mL	0	0	0.3±0.1*	0.7±0.1*†
Lung human AM, fmol/g tissue	0	0	11.9±0.6*	23.0±2.3*†

Control indicates MCT rats given culture medium; EPC, MCT rats given EPCs; AM-EPC, MCT rats given AM-expressing EPCs; and RV, right ventricular. Data are mean±SEM.

* $P<0.05$ vs control; † $P<0.05$ vs EPC.

dium after acute myocardial infarction.⁶ These findings suggest that progenitor cells have the ability to sense injured tissues. In fact, in the present study, intravenously administered GFP-expressing EPCs were incorporated into pulmonary arterioles and capillaries in MCT rats and differentiated mature endothelial cells. MCT injures endothelial cells of small arteries and capillaries in the lungs, resulting in pulmonary hypertension.¹⁹ Taking these findings together, transplanted EPCs may circulate in the blood and attach to injured pulmonary endothelia in MCT rats. Thus, EPCs may serve not only as a vehicle for gene delivery to injured pulmonary endothelia but also as a tissue-engineering tool in restoring intact pulmonary endothelium. Transplantation of EPCs without gene modification slightly but significantly decreased pulmonary vascular resistance in MCT rats. EPCs have been shown to express endothelial nitric oxide synthase and produce nitric oxide.¹⁴ In the present study, we showed that EPCs produce AM even when its gene is not transduced. These results suggest that vasodilator substances secreted from EPCs contribute to improvement in pulmonary hypertension.

We also investigated whether transplantation of gene-modified EPCs causes additional improvement in pulmonary hemodynamics and survival in MCT rats. AM is one of the most potent vasodilators synthesized by vascular endothelial cells.¹ Interestingly, EPCs cultured with AM DNA-gelatin complexes markedly secreted AM protein for more than 16 days. These results suggest relatively long-lasting AM secretion from EPCs. The consequence of this synthesis in MCT rats was a marked decrease in mean pulmonary arterial pressure and pulmonary vascular resistance. Histological examination revealed that transplantation of AM-expressing EPCs inhibited an increase in medial wall thickness of pulmonary arteries. Expectedly, transplantation of AM-expressing EPCs caused significantly greater improvement in pulmonary hypertension and vascular remodeling than transplantation of EPCs alone. Given the known potent vasoprotective effects of AM, such as vasodilation and inhibition of smooth muscle cell proliferation,^{1,20} it is interesting to speculate that AM secreted from EPCs may act not only as a circulating factor but also as an autocrine/paracrine factor in the regulation of pulmonary vascular tone and vascular

remodeling in MCT rats. Importantly, a single transplantation of AM-expressed EPCs improved survival in MCT rats compared with administration of EPCs alone or culture medium. These results suggest that ex vivo gene transfer into EPCs greatly enhances the therapeutic effects of EPC transplantation. Additional studies are necessary to examine whether repeated administration of EPCs produces an even greater effect than single transplantation.

Conclusions

Human umbilical cord blood-derived EPCs have a phagocytosing action that allows nonviral, highly efficient gene transfer into EPCs. Transplantation of AM DNA-transduced EPCs causes significantly greater improvement in pulmonary hypertension and better survival in MCT rats than transplantation of EPCs alone. Thus, the novel hybrid cell-gene therapy based on the phagocytosing action of EPCs may be a new therapeutic strategy for the treatment of pulmonary hypertension.

Acknowledgments

This work was supported by a grant from the Japan Cardiovascular Research Foundation; HLSRG-RAMT-nano-001 and -RHGTEFB-genome-005, RGCD13C-1 from the Ministry of Health, Labour, and Welfare (MHLW); grants from NEDO; a grant-in-aid for scientific research from the Ministry of Education, Culture, Sports, Science, and Technology (13470154 and 13877114); the Promotion of Fundamental Studies in Health Science of the Organization for Pharmaceutical Safety and Research (OPSR) of Japan; and a grant for Research on Human Genome, Tissue Engineering Food Biotechnology, application of cord blood for blood transplantation and tissue engineering from MHLW. We thank Dr Atsuhiko Kawamoto for his technical assistance.

References

1. Kitamura K, Kangawa K, Kawamoto M, et al. Adrenomedullin: a novel hypotensive peptide isolated from human pheochromocytoma. *Biochem Biophys Res Commun*. 1993;192:553-560.
2. Archer S, Rich S. Primary pulmonary hypertension: a vascular biology and translational research "work in progress." *Circulation*. 2000;102:2781-2791.
3. Asahara T, Murohara T, Sullivan A, et al. Bone marrow origin of endothelial progenitor cells responsible for postnatal vasculogenesis in physiological and pathological neovascularization. *Science*. 1997;275:965-967.

4. Takahashi T, Kalka C, Masuda H, et al. Ischemia- and cytokine-induced mobilization of bone marrow-derived endothelial progenitor cells for neovascularization. *Nat Med.* 1999;5:434-438.
5. Gill M, Dias S, Hattori K, et al. Vascular trauma induces rapid but transient mobilization of VEGFR2(+)/AC133(+) endothelial precursor cells. *Circ Res.* 2001;88:167-174.
6. Kawamoto A, Gwon HC, Iwaguro H, et al. Therapeutic potential of ex vivo expanded endothelial progenitor cells for myocardial ischemia. *Circulation.* 2001;103:634-637.
7. Tabata Y, Nagano A, Ikada Y. Biodegradation of hydrogel carrier incorporating fibroblast growth factor. *Tissue Eng.* 1999;5:127-138.
8. Fukunaka Y, Iwanaga K, Morimoto K, et al. Controlled release of plasmid DNA from cationized gelatin hydrogels based on hydrogel degradation. *J Control Release.* 2002;80:333-343.
9. Tabata Y, Ikada Y. Macrophage activation through phagocytosis of muramyl dipeptide encapsulated in gelatin microspheres. *J Pharm Pharmacol.* 1987;39:698-704.
10. Owji AA, Smith DM, Coppock HA, et al. An abundant and specific binding site for the novel vasodilator adrenomedullin in the rat. *Endocrinology.* 1995;136:2127-2134.
11. Yoshiyoshi M, Kamiya T, Kitamura K, et al. Plasma levels of adrenomedullin in primary and secondary pulmonary hypertension in patients <20 years of age. *Am J Cardiol.* 1997;79:1556-1558.
12. Nagaya N, Satoh T, Nishikimi T, et al. Hemodynamic, renal and hormonal effects of adrenomedullin infusion in patients with congestive heart failure. *Circulation.* 2000;101:498-503.
13. Nagaya N, Nishikimi T, Uematsu M, et al. Haemodynamic and hormonal effects of adrenomedullin in patients with pulmonary hypertension. *Heart.* 2000;84:653-658.
14. Murohara T, Ikeda H, Duan J, et al. Transplanted cord blood-derived endothelial precursor cells augment postnatal neovascularization. *J Clin Invest.* 2000;105:1527-1536.
15. Kalka C, Masuda H, Takahashi T, et al. Vascular endothelial growth factor (165) gene transfer augments circulating endothelial progenitor cells in human subjects. *Circ Res.* 2000;86:1198-1202.
16. Dimmeler S, Aicher A, Vasa M, et al. HMG-CoA reductase inhibitors (statins) increase endothelial progenitor cells via the PI 3-kinase/Akt pathway. *J Clin Invest.* 2001;108:391-397.
17. Kalka C, Masuda H, Takahashi T, et al. Transplantation of ex vivo expanded endothelial progenitor cells for therapeutic neovascularization. *Proc Natl Acad Sci U S A.* 2000;97:3422-3427.
18. Priller J, Flugel A, Wehner T, et al. Targeting gene-modified hematopoietic cells to the central nervous system: use of green fluorescent protein uncovers microglial engraftment. *Nat Med.* 2001;7:1356-1361.
19. Rosenberg H, Rabinovitch M. Endothelial injury and vascular reactivity in monocrotaline pulmonary hypertension. *Am J Physiol.* 1988;255:H1484-H1491.
20. Horio T, Kohno M, Kano H, et al. Adrenomedullin as a novel anti-migration factor of vascular smooth muscle cells. *Circ Res.* 1995;77:660-664.

Inhibition of cholinesterase elicits muscarinic receptor-mediated synaptic transmission in the rat adrenal medulla

Tsuyoshi Akiyama^{a,*}, Toji Yamazaki^a, Hidezo Mori^a, Kenji Sunagawa^b

^aDepartment of Cardiac Physiology, National Cardiovascular Center Research Institute, 5-7-1 Fujishiro-dai, Suita, Osaka, 565-8565 Japan

^bDepartment of Cardiovascular Dynamics, National Cardiovascular Center Research Institute, Suita, Osaka, 565-8565 Japan

Received 6 September 2002; received in revised form 12 November 2002; accepted 25 November 2002

Abstract

To determine the role of acetylcholinesterase in cholinergic synaptic transmission in the adrenal medulla *in vivo*, we applied a dialysis technique to the adrenal medulla of anesthetized rats and examined the effect of acetylcholinesterase inhibitor on the contribution of nicotinic and muscarinic receptors to catecholamine release. Exogenous acetylcholine-induced epinephrine release was inhibited by atropine (a muscarinic receptor antagonist) as well as hexamethonium (a nicotinic receptor antagonist). Endogenous acetylcholine (nerve stimulation)-induced epinephrine release was inhibited by hexamethonium but not atropine. In the presence of neostigmine (an acetylcholinesterase inhibitor), both exogenous and endogenous acetylcholine-induced catecholamine release was enhanced. In either case, epinephrine release was inhibited by atropine as well as hexamethonium. In the presence of eserine (another acetylcholinesterase inhibitor), endogenous acetylcholine-induced epinephrine release was also inhibited by atropine. Exogenous or endogenous acetylcholine-induced norepinephrine release was primarily inhibited by hexamethonium regardless of whether neostigmine was absent or present. In the rat adrenal medulla, the inhibition of acetylcholinesterase not only enhanced cholinergic synaptic transmission but also elicited muscarinic receptor-mediated synaptic transmission for epinephrine release.

© 2003 Elsevier B.V. All rights reserved.

Keywords: Microdialysis; Acetylcholine; Norepinephrine; Epinephrine; Nicotinic receptors

1. Introduction

In vivo catecholamine release from adrenal medulla is controlled by the central nervous system through the sympathetic pathway via splanchnic nerves, which make synaptic contacts with chromaffin cells (Coupland, 1965). It has been reported that catecholamine release induced by splanchnic nerve stimulation is predominantly inhibited by nicotinic receptor antagonists and is resistant to muscarinic receptor antagonists in dogs (Kennedy et al., 1991; Kimura et al., 1992), cats (Alamo et al., 1991) and rats (Wakade and Wakade, 1983). Acetylcholine released from splanchnic nerve endings evokes catecholamine release mainly by activation of nicotinic receptors on the surface of chromaffin cells. On the other hand, both nicotinic and muscarinic receptors are present on the surface

of chromaffin cells of various species because both receptor agonists evoke a substantial catecholamine release (Tsujimoto and Nishikawa, 1975; Kirpekar et al., 1982; Role and Perlman, 1983; Ballesta et al., 1989; Chen and Dixon, 1990; Chritton et al., 1991; Zhou et al., 1991). These findings have suggested that nicotinic receptors are primarily concentrated in the synaptic regions of chromaffin cells and muscarinic receptors localize on the extra-synaptic regions of chromaffin cells (Wakade and Wakade, 1983; Kimura et al., 1992). This anatomical distribution of receptors may explain the predominance of nicotinic receptors in physiological synaptic transmission. However, here, questions arise. Can acetylcholine go in and out at synaptic connections? What conditions are relevant to the extra-synaptic muscarinic receptor-mediated transmission in the *in vivo* adrenal medulla?

The action of released neurotransmitters is generally terminated by reuptake mechanisms through neuronal transporters or by enzymatic destruction. Released acetylcholine is degraded to choline and acetate by acetylcholinesterase, and choline but not acetylcholine is carried into the nerve

* Corresponding author. Tel.: +81-6-6833-5012x2380; fax: +81-6-6872-8092.

E-mail address: takiyama@ri.ncvc.go.jp (T. Akiyama).

endings through neuronal transporters. Thus, acetylcholinesterase plays a critical role in terminating the action of released acetylcholine. Under physiological conditions, there is enough acetylcholinesterase activity in splanchnic nerve endings, chromaffin cells and interstitial cells (Coup-land, 1965; Palkama, 1967; Lewis and Shute, 1969; Somogyi et al., 1975). Acetylcholine released from splanchnic nerve endings may be rapidly degraded before reaching the extra-synaptic muscarinic receptors. It has been, however, reported that exposure to chronic or acute stresses reduces acetylcholinesterase activity in the adrenal gland (Gabriel and Soliman, 1983). If acetylcholinesterase activity is reduced in the adrenal medulla, released acetylcholine may not only accumulate in synaptic regions of chromaffin cells but also spill over to the extra-synaptic regions. Then, we considered that acetylcholinesterase plays an important role in determining cholinergic receptors involved in the *in vivo* synaptic transmission.

In the present study, we applied the microdialysis technique to the adrenal medulla of anesthetized rats and tried to examine the role of acetylcholinesterase in the *in vivo* cholinergic synaptic transmission. First, we investigated the contribution of nicotinic and muscarinic receptors to exogenous or endogenous acetylcholine-induced catecholamine release. Second, we investigated the influence of acetylcholinesterase inhibitor on their contributions to exogenous or endogenous acetylcholine-induced catecholamine release.

2. Materials and methods

2.1. Animal preparation

The investigation conforms with the Guide for the Care and Use of Laboratory Animals published by the US National Institutes of Health (NIH Publication No. 85-23, revised 1996). Adult male Wistar rats weighing 340–480 g were anesthetized with pentobarbital sodium (50–55 mg·kg⁻¹ i.p.). The level of anesthesia was maintained with a continuous intravenous infusion of pentobarbital sodium (15–25 mg·kg⁻¹·h⁻¹ i.v.). A cervical midline incision was made to expose the trachea, which was then cannulated. The rats were ventilated with a constant-volume respirator using room air mixed with oxygen. A thermostatic heating pad was used to keep the esophageal temperature within a range of 37–38 °C. Heart rate, arterial pressure and electrocardiogram were monitored and recorded continuously. With the animal in the lateral position, the left adrenal gland and left splanchnic nerve were exposed by a flank incision, and the left splanchnic nerve was transected in all protocols. In protocols requiring nerve stimulation, shielded bipolar stainless steel electrodes were applied to the distal end of the nerve, which was then stimulated with a digital stimulator (SEN-7203, Nihon Kohden, Japan) with a rectangular pulse (10 V and 1 ms in duration).

2.2. Dialysis probe construction

The materials of the dialysis probe were the same as those used in our previous cardiac dialysis experiments (Akiyama and Yamazaki, 2001). Briefly, each end of the dialysis fiber (0.31 mm OD and 0.20 mm ID; PAN-1200 50,000 MW cutoff, Asahi Chemical, Japan) was inserted into the polyethylene tube (25-cm length, 0.5 mm OD and 0.2 mm ID; SP-8) and glued. The length of the dialysis fiber exposed was 3 mm. When a dialysis probe was bathed in 38 °C Ringer's solution containing norepinephrine (100 ng·ml⁻¹) and epinephrine (100 ng·ml⁻¹) and perfused with Ringer's solution at a speed of 10 µl·min⁻¹, *in vitro* recovery rates of norepinephrine and epinephrine were 1.7 ± 0.2% and 1.9 ± 0.3%, respectively (number of dialysis probes = 3).

2.3. *In vivo* dialysis technique

The left adrenal gland was gently lifted, and the dialysis probe was implanted in the medulla of the left adrenal gland along the long axis by using a fine guiding needle (10 mm length, 0.51 mm OD and 0.25 mm ID). The dialysis probe was perfused with Ringer's solution or Ringer's solution containing pharmacological agents at a speed of 10 µl·min⁻¹ using a microinjection pump (CMA/100, Carnegie Medicin, Sweden). Ringer's solution consisted of (in mM) 147.0 NaCl, 4.0 KCl and 2.25 CaCl₂. All pharmacological agents tested were locally administered by perfusion through the dialysis probe after being dissolved in Ringer's solution. The concentrations of pharmacological agents were determined based on their concentrations used in earlier *in vitro* studies and the *in vitro* recovery rate of the dialysis probe. One sampling period was 1 min (1 sample volume = 10 µl). Each sample was collected in a microtube containing 2 µl of 0.1N hydrochloric acid to prevent the oxidation of amine. In this study, catecholamine release was evoked by 1-min local administration of cholinergic receptor agonists or 1-min electrical stimulation of left splanchnic nerves. We continuously collected five dialysate samples per pharmacological or electrical stimulation: one before, one during and three after stimulation.

We measured the dead space volume for local administration or dialysate sampling. Taking this space into account, we locally administered pharmacological agents and sampled dialysate. Dialysate norepinephrine and epinephrine concentrations were high immediately after probe implantation, but decreased rapidly and stabilized within 3–4 h. After basal dialysate norepinephrine and epinephrine concentrations reached steady levels, we started the protocols.

Using high-performance liquid chromatography with electrochemical detection, dialysate norepinephrine and epinephrine concentrations were measured as indices of norepinephrine and epinephrine release. The dialysate sample from the adrenal medulla was injected directly into the high-performance liquid chromatography using an autosampler

(CMA/200, 240, Carnegie Medicin). Details of the high-performance liquid chromatography system have been previously described (Yamazaki et al., 1995).

2.4. Preliminary experiments

Preliminarily, to ensure that catecholamine release was reproducible on repetition of the same stimulation, we examined dialysate catecholamine levels in response to the repeated pharmacological or electrical stimulation: 1-min local administration of acetylcholine (1 mM) ($n=2$) or 1-min electrical stimulation of left splanchnic nerves (4 Hz) ($n=2$). Both stimulations were repeated six times at 30-min intervals. Substantial amounts of norepinephrine and epinephrine were observed in dialysate before stimulation. These basal levels were maintained throughout the experiment. Each stimulation elicited almost identical dialysate catecholamine responses on repetition. Dialysate norepinephrine and epinephrine levels reached peak levels during stimulation and declined after the stimulation was stopped. Based on these results, in the following main experiments, we repeated 1-min local administration of cholinergic receptor agonists or 1-min nerve stimulation and examined the dialysate catecholamine responses in various conditions.

2.5. Main experiments

2.5.1. Protocol 1

To ensure the presence of nicotinic or muscarinic receptors on the surface of rat chromaffin cells, we examined the dialysate catecholamine responses to a nicotinic or muscarinic receptor agonist. In six rats, the nicotinic receptor agonist, dimethylphenylpiperazinium or the muscarinic receptor agonist, pilocarpine was locally administered for 1 min at 30-min intervals. We tested 10 and 100 μM of dimethylphenylpiperazinium and 10 μM , 100 μM and 1 mM of pilocarpine.

2.5.2. Protocol 2

To determine the involvement of nicotinic and muscarinic receptors in catecholamine release, we examined the effect of cholinergic receptor antagonists on dialysate catecholamine responses to exogenous or endogenous acetylcholine: 1-min local administration of acetylcholine (1 mM) ($n=6$) or 1-min nerve stimulation at 2 ($n=4$) and 4 Hz ($n=6$). Each stimulation was repeated four times at 30-min intervals. The first and third stimulations were done as a control, and the second and fourth stimulations were done at 20-min local administration of the nicotinic receptor antagonist, hexamethonium (1 mM) or the muscarinic receptor antagonist, atropine (10 μM), respectively. Administration of each cholinergic receptor antagonist was stopped immediately after sampling. In addition, we examined the effect of combined nicotinic and muscarinic receptor antagonists on dialysate catecholamine responses to exogenous or endog-

enous acetylcholine: 1-min local administration of acetylcholine (1 mM) ($n=4$) or 1-min nerve stimulation at 2 ($n=3$) and 4 Hz ($n=4$). Each stimulation was repeated twice at 30-min intervals. The first stimulation was done as a control, and the second stimulation was done at 20-min local administration of combined hexamethonium and atropine.

2.5.3. Protocol 3

To determine the role of acetylcholinesterase in cholinergic synaptic transmissions, we examined the effects of acetylcholinesterase inhibitors on dialysate catecholamine responses to exogenous or endogenous acetylcholine: 1-min local administration of acetylcholine (10 μM) ($n=6$) or 1-min nerve stimulation at 2 Hz ($n=6$). The concentration of administered acetylcholine or the frequency of nerve stimulation was chosen to obtain similar dialysate catecholamine responses to those in protocol 2. Each stimulation was repeated five times at 30-min intervals. The first stimulation was done as a control in the absence of the acetylcholinesterase inhibitor. The remaining stimulations were done in the presence of the acetylcholinesterase inhibitor, neostigmine (10 μM), and the sequence of stimulations was the same as that in protocol 2. In four other rats, 1-min nerve stimulation (2 Hz) was similarly repeated, and another acetylcholinesterase inhibitor, eserine (100 μM) was tested to exclude the nonspecific effects of neostigmine.

At the end of the experiment, the rats were killed with pentobarbital sodium, and the implant sites were examined. The dialysis probes had been implanted in the adrenal gland medulla; no bleeding or necrosis was found macroscopically.

2.6. Statistical methods

To examine the effect of pharmacological agents and nerve stimulation, we analyzed heart rate and mean arterial blood pressure, and dialysate norepinephrine and epinephrine responses, by using one-way analysis of variance with repeated measures. When statistical significance was detected, the Newman–Keuls test was applied (Winer, 1971). Statistical significance was defined as $P<0.05$. The percentage was calculated for each animal and then averaged. Values are presented as means \pm S.E.

3. Results

Local administration of pharmacological agents did not influence heart rate or mean arterial pressure in any of the protocols. In protocol 2, the first nerve stimulation (4 Hz), at its maximum effect, decreased heart rate from 430 ± 7 to 414 ± 9 beats $\cdot\text{min}^{-1}$ and increased mean arterial blood pressure from 118 ± 7 to 133 ± 8 mm Hg ($P<0.05$). Mean arterial blood pressure and heart rate recovered after cessation of the nerve stimulation. Repeated nerve stimulation evoked the same responses of heart rate and mean arterial pressure.

Basal dialysate norepinephrine and epinephrine levels were not affected by cholinergic receptor antagonists or acetylcholinesterase inhibitors. In all sampling sequences, the peak dialysate norepinephrine or epinephrine levels were obtained during stimulation. We subtracted the basal value from the peak value of dialysate norepinephrine or epinephrine levels and expressed this value as an index of the dialysate norepinephrine or epinephrine response to stimulation.

3.1. Protocol 1

Local administration of dimethylphenylpiperazinium or pilocarpine increased dialysate norepinephrine and epinephrine concentrations, with these responses being dependent on the concentration of dimethylphenylpiperazinium or pilocarpine (Fig. 1). The ratios of norepinephrine response to epinephrine response were $79 \pm 11\%$ at $100 \mu\text{M}$ of dimethylphenylpiperazinium and $6 \pm 1\%$ at 1 mM of pilocarpine. None of the ratios were affected by the concentration of dimethylphenylpiperazinium or pilocarpine.

3.2. Protocol 2

3.2.1. Administration of acetylcholine

Local administration of acetylcholine increased dialysate norepinephrine and epinephrine concentrations (Fig. 2). The ratio of norepinephrine response to epinephrine response was $43 \pm 5\%$. In dialysate norepinephrine and epinephrine responses, there was no difference between the first and third stimulations. This indicated that the effect of hexamethonium had already disappeared 30 min after the cessation of local administration. Dialysate norepinephrine response was inhibited by hexamethonium but not by atropine. Dialysate epinephrine response was inhibited by atropine

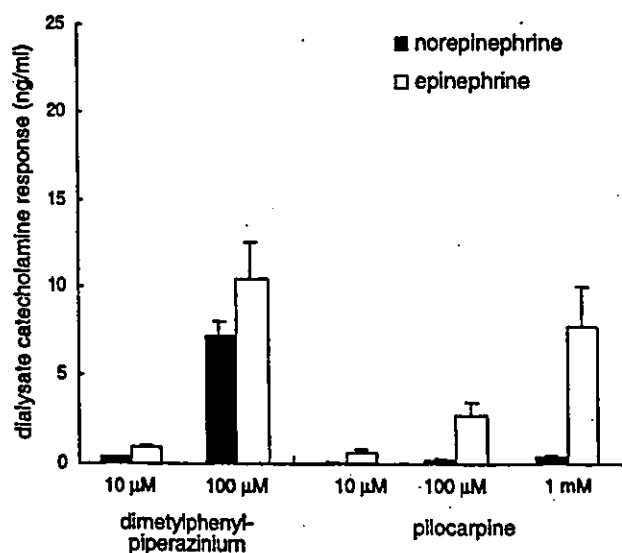


Fig. 1. Dialysate catecholamine response to dimethylphenylpiperazinium or pilocarpine. Values are means \pm S.E.

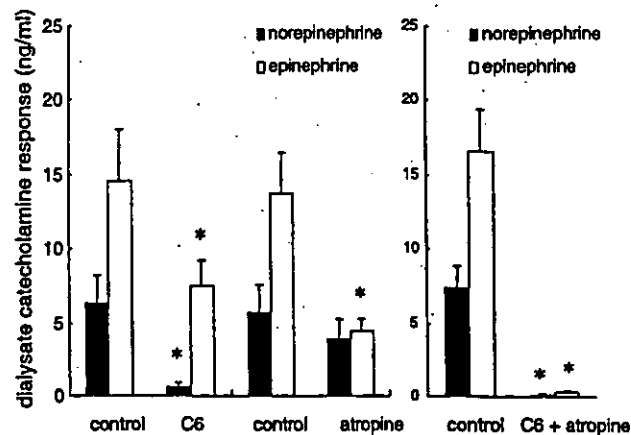


Fig. 2. Effects of hexamethonium (C6) and atropine on dialysate catecholamine response induced by administration of acetylcholine. Values are means \pm S.E. * $P < 0.05$ vs. dialysate norepinephrine or epinephrine response just before administration of C6 and/or atropine.

as well as hexamethonium. Both dialysate norepinephrine and epinephrine responses were completely inhibited by the combination of hexamethonium and atropine, and this inhibition of dialysate epinephrine response was almost equivalent to the sum of the individual inhibition by hexamethonium and atropine.

3.2.2. Nerve stimulation at 2 and 4 Hz

Nerve stimulation at both frequencies increased dialysate norepinephrine and epinephrine concentrations (Fig. 3). The ratio of norepinephrine response to epinephrine response was $14 \pm 3\%$ at 2 Hz and $24 \pm 3\%$ at 4 Hz stimulation. At both frequencies, the dialysate norepinephrine response was inhibited by hexamethonium but not by atropine. Dialysate epinephrine response was also inhibited by hexamethonium but not by atropine. The inhibition by the combination of hexamethonium and atropine was almost the same as that by hexamethonium alone.

3.3. Protocol 3

3.3.1. Administration of acetylcholine in the presence of neostigmine

Neostigmine enhanced dialysate norepinephrine and epinephrine responses by about 30–40-fold, but did not change the ratio of norepinephrine response to epinephrine response (Fig. 4). Dialysate norepinephrine response was inhibited by hexamethonium but not by atropine. Dialysate epinephrine response was inhibited by atropine as well as hexamethonium. Neostigmine did not alter the inhibitory action of hexamethonium or atropine.

3.3.2. Nerve stimulation in the presence of neostigmine and eserine

Neostigmine enhanced the dialysate norepinephrine and epinephrine responses by about two- to threefold, but did not change the ratio of norepinephrine response to epineph-

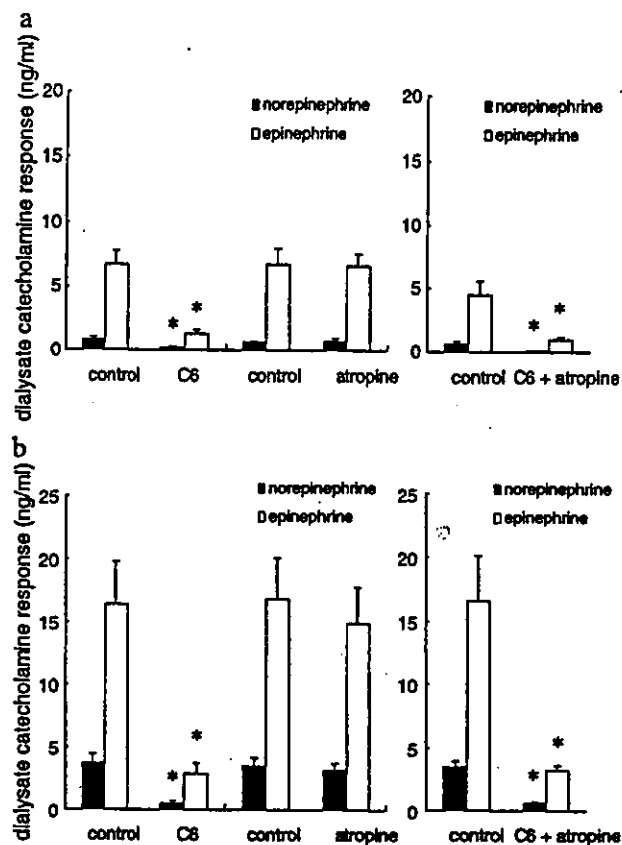


Fig. 3. Effects of hexamethonium (C6) and atropine on dialysate catecholamine response induced by nerve stimulation at 2 (a) and 4 Hz (b). Values are means \pm S.E. * P < 0.05 vs. dialysate norepinephrine or epinephrine response just before administration of C6 and/or atropine.

rine response (Fig. 5a). Dialysate norepinephrine response was inhibited by hexamethonium but not by atropine. Dialysate epinephrine response was inhibited by atropine as well as hexamethonium. Neostigmine elicited the mus-

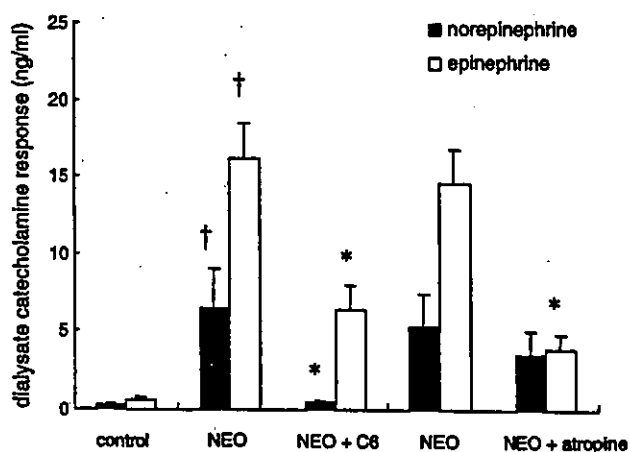


Fig. 4. Effect of hexamethonium (C6) or atropine on dialysate catecholamine response induced by administration of acetylcholine in the presence of neostigmine (NEO). Values are means \pm S.E. † P < 0.05 vs. dialysate norepinephrine or epinephrine response in the absence of NEO. * P < 0.05 vs. dialysate norepinephrine or epinephrine response just before administration of C6 or atropine.

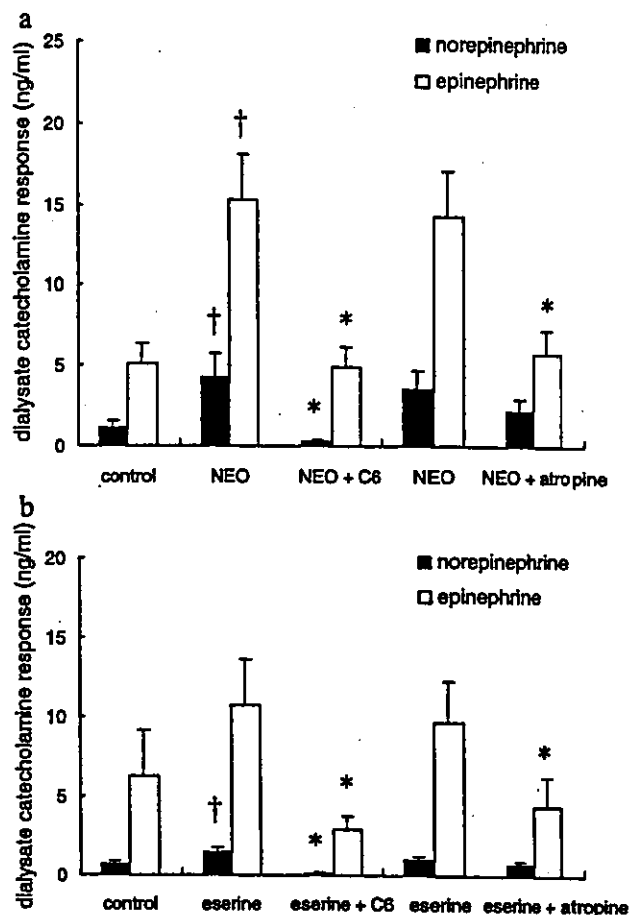


Fig. 5. Effect of hexamethonium (C6) or atropine on dialysate catecholamine response induced by nerve stimulation in the presence of neostigmine (NEO) (a) or eserine (b). Values are means \pm S.E. † P < 0.05 vs. dialysate norepinephrine or epinephrine response in the absence of NEO or eserine. * P < 0.05 vs. dialysate norepinephrine or epinephrine response just before administration of C6 or atropine.

carinic receptor-mediated synaptic transmission, and the inhibitory action of hexamethonium or atropine became identical with that of exogenous acetylcholine. Enhancement of dialysate norepinephrine and epinephrine responses by eserine was smaller than that by neostigmine, but changes in the inhibitory actions of hexamethonium or atropine were similar to that by neostigmine (Fig. 5b).

3.3.3. Time course of dialysate catecholamine levels in the absence and presence of neostigmine

To examine the influence of neostigmine on the decay of catecholamine release induced by exogenous or endogenous acetylcholine, we compared the time course of dialysate catecholamine levels in the absence and presence of neostigmine (Fig. 6). In 10 μ M acetylcholine with neostigmine, the peak value and decay-slope of dialysate catecholamine levels corresponded to those in 1 mM acetylcholine. Similarly, the peak value and decay-slope of dialysate catecholamine levels were almost identical between 2 Hz stimulation with neostigmine and 4 Hz stimulation. Neostigmine en-

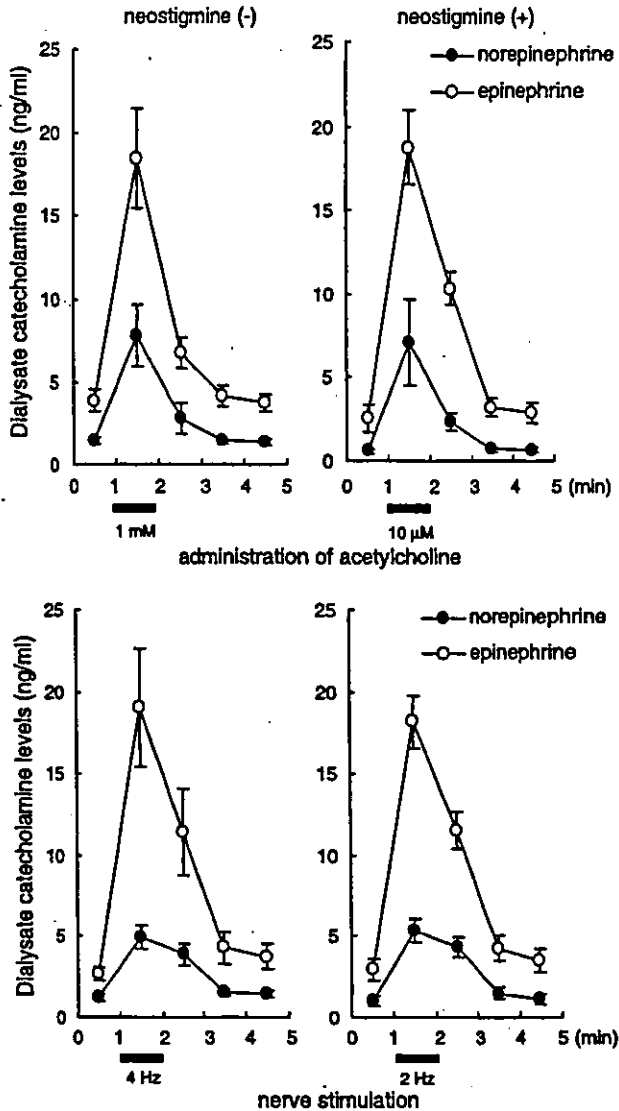


Fig. 6. Comparison of exogenous and endogenous acetylcholine-induced changes in dialysate catecholamine levels in the absence and presence of neostigmine.

hanced the exogenous or endogenous acetylcholine-induced dialysate catecholamine response, but did not change the decay-slope in dialysate catecholamine levels.

4. Discussion

Microdialysis technique with high-performance liquid chromatography made it possible to continuously monitor norepinephrine and epinephrine release at 1-min intervals without blood sampling in the *in vivo* rat adrenal medulla. Moreover, we were able to locally administer pharmacological agents and observe their effects on catecholamine release without systemic influence. Thus, dialysate sampling with local administration enabled us to precisely assess the cholinergic transmission in the adrenal medulla.

4.1. Presence of nicotinic and muscarinic receptors on the surface of chromaffin cells

In our study of rat adrenals, a nicotinic receptor agonist (dimethylphenylpiperazinium) substantially evoked both norepinephrine and epinephrine release, while a muscarinic receptor agonist (pilocarpine) primarily evoked epinephrine release only. Our observations are consistent with earlier studies in the perfused rat adrenal gland (Wakade and Wakade, 1983; Chen and Dixon, 1990; Zhou et al., 1991). It is well known that adrenal chromaffin cells are divided into two types of populations: norepinephrine- and epinephrine-storing cells (Coupland, 1984). Therefore, in the rat adrenal medulla, both nicotinic and muscarinic receptors substantially exist on the surface of epinephrine-storing cells, while on the surface of norepinephrine-storing cells, nicotinic receptors are primarily present, but muscarinic receptors may be nearly absent.

4.2. Contribution of nicotinic and muscarinic receptors to catecholamine release

Exogenous acetylcholine-induced norepinephrine release was predominantly mediated by nicotinic receptors, while exogenous acetylcholine-induced epinephrine release was mediated by muscarinic as well as nicotinic receptors. These data also support the findings from earlier studies (Wakade and Wakade, 1983; Chen and Dixon, 1990; Zhou et al., 1991) and our agonist study in protocol 1. On the other hand, endogenous acetylcholine-induced norepinephrine and epinephrine release was exclusively mediated by nicotinic receptors. Involvement of muscarinic receptors was not significant in either norepinephrine or epinephrine release.

There was a differential contribution of nicotinic and muscarinic receptors between exogenous and endogenous acetylcholine-induced epinephrine release. Cholinergic synaptic transmission by endogenous acetylcholine was exclusively mediated by nicotinic receptors. Our observations agree with earlier studies in rats (Wakade and Wakade, 1983) and dogs (Kimura et al., 1992). Splanchnic nerves densely innervate the adrenal medulla, and their endings make synaptic contacts with chromaffin cells (Coupland, 1965). If exogenous acetylcholine equally reaches the synaptic and extra-synaptic regions of chromaffin cells while endogenous acetylcholine acts and terminates in the synaptic regions, nicotinic receptors could be primarily localized at synaptic regions and muscarinic receptors could be present on the extra-synaptic regions of the epinephrine-storing chromaffin cells. Actually, nicotinic receptors are concentrated at the neuromuscular junction of innervated skeletal muscle (Apel and Merlie, 1995) and at synaptic zones of postsynaptic membranes in sympathetic ganglia (Marshall, 1981) and brain neurons (Arroyo-Jiménez et al., 1999). Moreover, immunohistochemical analysis of guinea-pig chromaffin cells recently revealed that nicotinic receptors were mainly concentrated at synaptic

regions (Inoue et al., 2000). Thus, this anatomical localization of receptors may explain the difference in the contribution of cholinergic receptors between exogenous and endogenous acetylcholine-induced catecholamine release. Here, we focused on whether synaptic connection is so tight that released acetylcholine cannot spill over to extra-synaptic regions and on what conditions are relevant to the muscarinic receptor-mediated cholinergic transmission in the *in vivo* state. We concentrated on the enzymatic degradation by acetylcholinesterase.

4.3. Influence of acetylcholinesterase inhibitor on catecholamine release

Acetylcholinesterase inhibitors enhance the exogenous or endogenous acetylcholine-induced catecholamine release response in the adrenal medulla (Tsujimoto and Nishikawa, 1975; Orts et al., 1987). This enhancement may be ascribed to the elevation of acetylcholine levels on the surface of chromaffin cells, the reduction in the decay-slope of acetylcholine levels, and/or the spread of the action site of acetylcholine. In the present study monitoring at 1-min intervals, neostigmine enhanced the exogenous or endogenous acetylcholine-induced catecholamine release response, but did not change the decay-slope of catecholamine release. Thus, it is unlikely that enhancement of the catecholamine release response is attributable to the slow decay of acetylcholine levels on the surface of chromaffin cells.

Neostigmine caused a 30–40-fold increase in the exogenous acetylcholine-induced catecholamine release. This enhancement was much greater than that in the endogenous acetylcholine-induced catecholamine release response. There is abundant acetylcholinesterase activity on splanchnic nerve endings, chromaffin cells and interstitial cells (Coupland, 1965; Palkama, 1967; Lewis and Shute, 1969; Somogyi et al., 1975). Our data suggest that about 97% of administered acetylcholine was degraded by tissue acetylcholinesterase without reaching cholinergic receptors on the surface of chromaffin cells, and only about 3% of administered acetylcholine was bound to cholinergic receptors, leading to catecholamine release. Moreover, the catecholamine release response and the manner of contribution of cholinergic receptors were almost identical between 10 μ M acetylcholine in the presence of neostigmine and 1 mM acetylcholine in the absence of neostigmine. Therefore, in the case of exogenously administered acetylcholine, acetylcholinesterase inhibitor equally elevates acetylcholine levels on the surface of chromaffin cells regardless of synaptic or extra-synaptic regions.

Neostigmine caused a three- to fivefold increase in the endogenous acetylcholine-induced catecholamine release and changed the manner of contribution of cholinergic receptors to epinephrine release. Epinephrine release by nerve stimulation in the absence of neostigmine was exclusively mediated by nicotinic receptors, but epinephrine release by nerve stimulation in the presence of neostigmine

was mediated by muscarinic as well as nicotinic receptors. In the presence of neostigmine, the manner of contribution of cholinergic receptors to endogenous acetylcholine-induced catecholamine release was similar to that to exogenous acetylcholine-induced catecholamine release. We also obtained similar results in the presence of another acetylcholinesterase inhibitor, eserine. Thus, acetylcholinesterase inhibitors not only enhanced the endogenous acetylcholine-induced catecholamine release response but also elicited muscarinic receptor-mediated epinephrine release. The epinephrine release response induced by 2 Hz stimulation in the presence of neostigmine was almost identical to that induced by 4 Hz stimulation in the absence of neostigmine. Thus, the amount of acetylcholine contributing to epinephrine release could be also similar between the two stimulations. The manner of contribution of cholinergic receptors was, however, different between the absence and presence of neostigmine. This difference could not be explained by elevation of the acetylcholine level in the synaptic regions. Recently, an electrophysiological study in the rat ganglion suggested that synaptically released acetylcholine activated the receptors located extra-synaptically in the presence of eserine (Callister and Sah, 1997). Considering that muscarinic receptors are mainly present on the extra-synaptic regions of epinephrine-storing cells, our data indicate that acetylcholinesterase inhibitors extend the binding sites of endogenous acetylcholine to the extra-synaptic regions rather than elevate the acetylcholine level in the synaptic regions and elicit muscarinic receptor-mediated synaptic transmission.

4.4. Other possible mechanisms

It has been reported that ganglionic acetylcholine release receives presynaptic autoinhibition through muscarinic receptors (Dujic et al., 1990; Myers and Undem, 1996). Moreover, an electrophysiological study suggested that the acetylcholine release from splanchnic nerves received presynaptic inhibition through muscarinic receptors in rat adrenal gland (Barbara et al., 1998). If so, acetylcholinesterase inhibitors would induce the activation of presynaptic muscarinic receptors by increasing the acetylcholine level in synaptic regions (Brehm et al., 1992). In such a condition, a muscarinic receptor antagonist would facilitate acetylcholine release by blocking presynaptic autoinhibition and acting to facilitate norepinephrine and epinephrine release. Therefore, the inhibition by muscarinic receptor antagonists in the presence of acetylcholinesterase inhibitors cannot be explained by the presynaptic regulatory mechanism on splanchnic nerve endings.

It has been reported that cholinesterase inhibitors at high concentrations block nicotinic receptors in adrenal chromaffin cells (Mizobe and Livett, 1982), striatal synaptosomes (Clarke et al., 1994) and sympathetic neurons (Zheng et al., 1998). Moreover, it has been speculated that inactivation of nicotinic receptors enhances the sensitivity of muscarinic

receptors in the process of catecholamine release from the adrenal gland (Lee and Trendelenburg, 1967; Tsujimoto and Nishikawa, 1975). Neostigmine might block nicotinic receptors on the chromaffin cells and enhance the sensitivity of muscarinic receptors. This action might be involved in the cholinergic transmission through muscarinic receptors in the presence of acetylcholinesterase inhibitors. In our study, however, 10 μM neostigmine did not affect the contribution of nicotinic and muscarinic receptors to exogenous acetylcholine-induced catecholamine release. Thus, under our experimental conditions, it is unlikely that neostigmine blocks nicotinic receptors and enhances the sensitivity of muscarinic receptors.

In conclusion, in the *in vivo* state, acetylcholinesterase prevents the spillover of released acetylcholine to extra-synaptic regions and restricts its action to synaptic regions. Acetylcholinesterase inhibitor extends the action of released acetylcholine to the extra-synaptic regions and elicits the muscarinic receptor-mediated synaptic transmission. On the other hand, acetylcholinesterase prevents the administered acetylcholine from reaching the surface of chromaffin cells. Acetylcholinesterase inhibitor prevents degradation of administered acetylcholine and potentiates the effect of administered acetylcholine on nicotinic and muscarinic receptors on the surface of chromaffin cells regardless of location. Thus, acetylcholinesterase plays a crucial role in the differential contribution of cholinergic receptors to exogenous and endogenous acetylcholine-induced catecholamine release.

Acknowledgements

This study was supported by the Program for Promotion of Fundamental Studies in Health Science of the Organization for Pharmaceutical Safety and Research (of Japan), by a Health Sciences Research Grant for Advanced Medical Technology from the Ministry of Health and Welfare of Japan, by a Ground-Based Research Grant for the Space Utilization promoted by NASDA (National Space Development Agency of Japan) and Japan Space Forum, and by grants-in-aid for scientific research from the Ministry of Education, Science.

References

- Akiyama, T., Yamazaki, T., 2001. Myocardial interstitial norepinephrine and dihydroxyphenylglycol levels during ischemia and reperfusion. *Cardiovasc. Res.* 49, 78–85.
- Alamo, L., Garcia, A.G., Borges, R., 1991. Electrically-evoked catecholamine release from cat adrenals. *Biochem. Pharmacol.* 42, 973–978.
- Apel, E.D., Merlie, J.P., 1995. Assembly of the postsynaptic apparatus. *Curr. Opin. Neurobiol.* 5, 62–67.
- Arroyo-Jiménez, M.M., Bourgeois, J.P., Marubio, L.M., Le Sourd, A.M.L., Ottersen, O.P., Rinvik, E., Fairén, A., Changeux, J.P., 1999. Ultrastructural localization of the $\alpha 4$ -subunit of the neuronal acetylcholine nicotinic receptor in the rat substantia nigra. *J. Neurosci.* 19, 6475–6487.
- Ballesta, J.J., Borges, R., Garcia, A.G., Hidalgo, M.J., 1989. Secretory and radioligand binding studies on muscarinic receptors in bovine and feline chromaffin cells. *J. Physiol.* 418, 411–426.
- Barbára, J.G., Lemos, V.S., Takeda, K., 1998. Pre- and post-synaptic muscarinic receptors in thin slices of rat adrenal gland. *Eur. J. Neurosci.* 10, 3535–3545.
- Brehm, G., Lindmar, R., Löffelholz, K., 1992. Inhibitory and excitatory muscarinic receptors modulating the release of acetylcholine from the postganglionic parasympathetic neuron of the chicken heart. *Naunyn-Schmiedeberg's Arch. Pharmacol.* 346, 375–382.
- Callister, R.J., Sah, P., 1997. The removal of acetylcholine by diffusion at nicotinic synapses in the rat otic ganglion. *J. Physiol.* 505, 165–175.
- Chen, Y.M., Dixon, W.R., 1990. The effect of etorphine on nicotinic- and muscarinic-induced catecholamine secretion from perfused rat adrenal glands. *Life Sci.* 46, 1167–1173.
- Critton, S.L., Dousa, M.K., Yaksh, T.L., Tyce, G.M., 1991. Nicotinic- and muscarinic-evoked release of canine adrenal catecholamines and peptides. *Am. J. Physiol.* 260, R589–R599.
- Clarke, P.B., Reuben, M., el-Bizri, H., 1994. Blockade of nicotinic responses by physostigmine, tacrine and other cholinesterase inhibitors in rat striatum. *Br. J. Pharmacol.* 111, 695–702.
- Coupland, R.E., 1965. *The Natural History of the Chromaffin Cell*. Longmans, London.
- Coupland, R.E., 1984. Ultrastructural features of the mammalian adrenal medulla. In: Motta, P.M. (Ed.), *Ultrastructure of Endocrine Cells and Tissues*. Nijhoff, Boston, MA, pp. 168–179.
- Dujic, Z., Roerig, D.L., Schedewie, H.K., Kampine, J.P., Bošnjak, Z.J., 1990. Presynaptic modulation of ganglionic ACh release by muscarinic and nicotinic receptors. *Am. J. Physiol.* 259, R288–R293.
- Gabriel, N.N., Soliman, K.F., 1983. Effects of stress on the acetylcholinesterase activity of the hypothalamus–pituitary–adrenal axis in the rat. *Horm. Res.* 17, 43–48.
- Inoue, M., Fujishiro, N., Ogawa, K., Muroi, M., Sakamoto, Y., Imanaga, I., Shioda, S., 2000. Pituitary adenylate cyclase-activating polypeptide may function as a neuromodulator in guinea-pig adrenal medulla. *J. Physiol.* 528, 473–487.
- Kennedy, J.G., Breslow, M.J., Tobin, J.R., Traystman, R.J., 1991. Cholinergic regulation of adrenal medullary blood flow. *Am. J. Physiol.* H1836–H1841.
- Kimura, T., Shimamura, T., Satoh, S., 1992. Effects of pirenzepine and hexamethonium on adrenal catecholamine release in responses to endogenous and exogenous acetylcholine in anesthetized dogs. *J. Cardiovasc. Pharmacol.* 20, 870–874.
- Kirpekar, S.M., Prat, J.C., Schiavone, M.T., 1982. Effect of muscarine on release of catecholamines from the perfused adrenal gland of the cat. *Br. J. Pharmacol.* 77, 455–460.
- Lee, F.L., Trendelenburg, U., 1967. Muscarinic transmission of preganglionic impulses to the adrenal medulla of the cat. *J. Pharmacol. Exp. Ther.* 158, 73–79.
- Lewis, P.R., Shute, C.C., 1969. An electron-microscopic study of cholinesterase distribution in the rat adrenal medulla. *J. Microsc.* 89, 181–193.
- Marshall, L.M., 1981. Synaptic localization of α -bungarotoxin binding which blocks nicotinic transmission at frog sympathetic neurons. *Proc. Natl. Acad. Sci.* 78, 1948–1952.
- Mizobe, F., Livett, B.G., 1982. Biphasic effect of eserine and other acetylcholinesterase inhibitors on the nicotinic response to acetylcholine in cultured adrenal chromaffin cells. *J. Neurochem.* 39, 379–385.
- Myers, A.C., Udem, B.J., 1996. Muscarinic receptor regulation of synaptic transmission in airway parasympathetic ganglia. *Am. J. Physiol.* 270, L630–L636.
- Orts, A., Orellana, C., Canto, T., Cena, V., Gonzalez-Garcia, C., Garcia, A.G., 1987. Inhibition of adrenomedullary catecholamine release by propranolol isomers and clonidine involving mechanisms unrelated to adrenoceptors. *Br. J. Pharmacol.* 92, 795–801.

- Palkama, A., 1967. Demonstration of adrenomedullary catecholamines and cholinesterase at electron microscopic level in the same tissue section. *Ann. Med. Exp. Biol. Fenn.* 45, 295–306.
- Role, L.W., Perlman, R.L., 1983. Both nicotinic and muscarinic receptors mediate catecholamine secretion by isolated guinea-pig chromaffin cells. *Neuroscience* 10, 979–985.
- Somogyi, P., Chubb, I.W., Smith, A.D., 1975. A possible structural basis for the extracellular release of acetylcholinesterase. *Proc. R. Soc. Lond., Ser. B: Biol. Sci.* 191, 271–283.
- Tsujimoto, A., Nishikawa, T., 1975. Further evidence for nicotinic and muscarinic receptors and their interaction in dog adrenal medulla. *Eur. J. Pharmacol.* 34, 337–344.
- Wakade, A.R., Wakade, T.D., 1983. Contribution of nicotinic and muscarinic receptors in the secretion of catecholamines evoked by endogenous and exogenous acetylcholine. *Neuroscience* 10, 973–978.
- Winer, B.J., 1971. *Statistical Principles in Experimental Design*, 2nd ed. McGraw-Hill, New York.
- Yamazaki, T., Akiyama, T., Shindo, T., 1995. Routine high-performance liquid chromatographic determination of myocardial interstitial norepinephrine. *J. Chromatogr., B: Biomed. Appl.* 670, 328–331.
- Zheng, J.Q., He, X.P., Yang, A.Z., Liu, C.G., 1998. Neostigmine competitively inhibited nicotinic acetylcholine receptors in sympathetic neurons. *Life Sci.* 62, 1171–1178.
- Zhou, X.F., Marley, P.D., Livett, B.G., 1991. Substance P modulates the time course of nicotinic but not muscarinic catecholamine secretion from perfused adrenal glands of rat. *Br. J. Pharmacol.* 104, 159–165.

Intense Characteristic X-ray Irradiation from Weakly Ionized Linear Plasma and Applications

Eiichi SATO, Yasuomi HAYASI^{*}, Rudolf GERMER^{**}, Etsuro TANAKA^{***}, Hidezo MORI^{****},
Toshiaki KAWAI^{*****}, Haruo OBARA^{*****}, Toshio ICHIMARU^{*****},
Kazuyoshi TAKAYAMA^{*****} and Hideaki IDO^{*****}

Department of Physics, Iwate Medical University, 3-16-1 Honchodori, Morioka 020-0015, Japan

^{*}Department of Electrical Engineering, Hachinohe National College of Technology,
16-1 Tamonoki Uwanotai, Hachinohe 039-1104, Japan

^{**}ITP, FHTW FB1 and TU-Berlin, Blankenhainer Str. 9, D 12249 Berlin, Germany

^{***}Department of Physiology, School of Medicine, Tokai University, Boseidai, Isehara 259-1193, Japan

^{****}Department of Cardiac Physiology, National Cardiovascular Center Research Institute,
5-7-1 Fujishiro-dai, Suita, Osaka 565-8565, Japan

^{*****}Electron Tube Division #2, Hamamatsu Photonics Inc., 314-5 Shimokanzo,
Toyooka Village, Iwata-gun 438-0193, Japan

^{*****}Department of Radiological Technology, College of Medical Science, Tohoku University,
1-1 Seiryochō, Sendai 980-0872, Japan

^{*****}Department of Radiological Technology, School of Health Sciences, Hirosaki University,
66-1 Honcho, Hirosaki 036-8564, Japan

^{*****}Shock Wave Research Center, Institute of Fluid Science, Tohoku University,
2-1-1 katahira, Aoba-ku, Sendai 980-8577, Japan

^{*****}Department of Applied Physics, Faculty of Engineering, Tohoku Gakuin University,
1-13-1 Chuo, Tagajo 985-0873, Japan

(Received June 9, 2002, in final form, April 28, 2003)

Abstract: In the plasma flash x-ray generator, a high-voltage main condenser of approximately 200 nF is charged up to 55 kV by a power supply, and electric charges in the condenser are discharged to an x-ray tube after triggering the cathode electrode. The flash x-rays are then produced. The x-ray tube is a demountable triode that is connected to a turbo molecular pump with a pressure of approximately 1 mPa. As electron flows from the cathode electrode are roughly converged to a rod target by electric field in the x-ray tube, the weakly ionized linear plasma, which consists of molybdenum ions and electrons, forms by target evaporation. At a charging voltage of 50 kV, the maximum tube voltage was almost equal to the charging voltage of the main condenser, and the peak current was about 20 kA. When the charging voltage was increased, the linear plasma formed, and the K-series characteristic x-ray intensities increased. The K lines were quite sharp and intense, and hardly any bremsstrahlung rays were detected. When a copper target was employed, the x-ray pulse widths were approximately 700 ns, and the time-integrated x-ray intensity had a value of approximately 30 $\mu\text{C}/\text{kg}$ at 1.0 m from the x-ray source with a charging voltage of 50 kV.

Key words: flash x-ray, characteristic x-ray, quasi-monochromatic x-ray, weakly ionized plasma, linear plasma, micro-angiography.

1. INTRODUCTION

Synchrotrons generate high-dose-rate monochroma-

tic x-rays utilizing silicon monochromators, and the x-ray photon energy is determined by Bragg's angle. These rays play an important role in parallel radiography and